Organometallics 1992, *11*, 2206–2211

Dimeric Structures of Di-*n*-butyltin(IV) Ortho-Substituted Dibenzoates

Suraj P. Narula,* Shashi K. Bharadwaj,[1] and Yash Sharda[1]

Department of Chemistry, Panjab University, Chandigarh-160014, India

Roberta O. Day, Lori Howe,[1] and Robert R. Holmes*

Department of Chemistry, University of Massachusetts, Amherst, Massachusetts 01003

Received November 3, 1991

Reaction of $(n\text{-Bu})_2\text{SnO}$ with ortho-substituted benzoic acids yielded the new tin(IV) derivatives $(n\text{-Bu})_2\text{Sn}(\text{O}_2\text{CC}_6\text{H}_4\text{-}o\text{-OH})_2$ (1) and $(n\text{-Bu})_2\text{Sn}(\text{O}_2\text{CC}_6\text{H}_4\text{-}o\text{-Cl})_2$ (2), whose X-ray analyses showed hydrogen bonding in 1 and long Sn–O bridges in 2, leading to dimeric formulations. Solid-state infrared and ^{119m}Sn Mössbauer spectral data indicate carboxylate stretching frequencies and coordination at tin consistent with the X-ray structures. Comparison of related dicarboxylate tin compositions with similar structures reveals a correlation showing an increase in the C–Sn–C angle as the intermolecular Sn–O bond length decreases. The hydroxyl derivative 1 provides the first example of a hydrogen-bridged dimer formation. The geometry at tin is discussed in terms of a bicapped tetrahedron with four normal covalent bonds (two Sn–O and two Sn–C bond distances) and two longer Sn–O distances. The former define the tetrahedra and the latter the capped faces. The hydroxy derivative 1 crystallizes in the monoclinic space group $P2_1/c$ with a = 9.345 (3) Å, b = 24.086 (5) Å, c = 10.839 (3) Å, β = 107.77 (2)°, and Z = 4. The chloro derivative 2 crystallizes in the monoclinic space group $P2_1/c$ with a = 12.369 (2) Å, b = 8.830 (2) Å, c = 22.114 (5) Å, β = 102.18 (2); and Z = 4. The final conventional unweighted residuals are 0.038 (1) and 0.028 (2).

Introduction

Only recently have structures of diorganotin(IV) dicarboxylates appeared despite their importance in industrial applications, e.g., as PVC stabilizers[2] and catalysts for a variety of reactions.[3,4] The first structural reports concerned the acetate, $\text{Me}_2\text{Sn}(\text{O}_2\text{CCH}_3)_2$ (A),[5] and the *p*-aminobenzoate, $\text{Me}_2\text{Sn}(\text{O}_2\text{CC}_6\text{H}_4\text{-}p\text{-NH}_2)_2$ (B),[6] derivatives, which were shown by X-ray analysis to have similar distorted octahedral geometries in a monomeric arrangement. An additional monomeric structure was found in the *p*-bromobenzoate, $(n\text{-Bu})_2\text{Sn}(\text{O}_2\text{CC}_6\text{H}_4\text{-}p\text{-Br})_2$ (C).[7] In contrast, X-ray analysis of the di-*n*-butyltin(IV) di-*o*-bromobenzoate derivative, $(n\text{-Bu})_2\text{Sn}(\text{O}_2\text{CC}_6\text{H}_4\text{-}o\text{-Br})_2$ (D),[8] revealed a weakly bridged dimeric arrangement.

To assess the prevalence of these structural types, we report the molecular structures of the related derivatives, $(n\text{-Bu})_2\text{Sn}(\text{O}_2\text{CC}_6\text{H}_4\text{-}o\text{-OH})$ (1) and $(n\text{-Bu})_2\text{Sn}(\text{O}_2\text{CC}_6\text{H}_4\text{-}o\text{-Cl})$ (2), along with ^{119m}Sn Mössbauer, mass spectral, and infrared data. The hydroxy derivative 1 introduces hydrogen bonding as a structural influence, while the chloro derivative 2 allows the examination of an electronegativity change neighboring the coordination site.

Experimental Section

Spectroscopy. IR spectra were recorded on KBr pellets with a Perkin-Elmer 621 spectrophotometer. The ^{119m}Sn Mössbauer spectra were obtained at 77 K using a Harwell spectrophotometer equipped with a 256-multichannel analyzer and a Ba $^{119m}\text{SnO}_3$ source. Least-squares method was used for data reduction of the Lorentzian line shape. Elemental analyses were obtained using a CARLO ERBA STRUMENTZIONE (ITALY) elemental analyzer Model 1106.

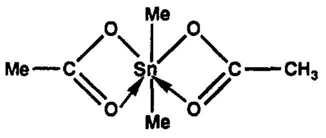

A

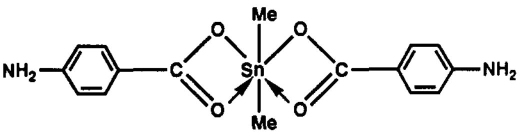

B

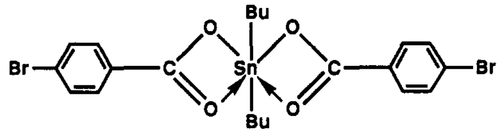

C

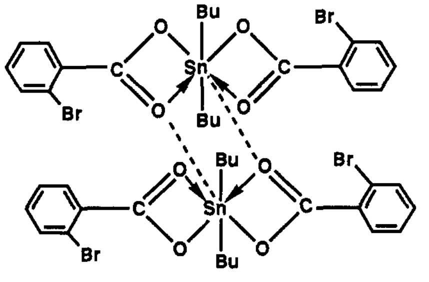

D

Mass spectral measurements were carried out on a V-G Micromass MM 70/70F double-focusing spectrophotometer with 70°/12.7 on the electrostatic and magnetic analyzer.

---

[1] This work represents in part a portion of the Ph.D. Theses of Shaski K. Bharadwaj and Yash Sharda, Panjab University, Chandigarh-160014, India, and in part a portion of the M.S. Thesis of Lori Howe, University of Massachusetts, Amherst, MA, 1990.

[2] Davis, A. G.; Smith, P. J. In *Comprehensive Organometallic Chemistry*; Wilkinson, G., Stone, F. G. A., Abel, E. W., Eds.; Pergamon: New York, 1982; Vol. 2, pp 610–616 and references cited therein.

[3] Gross, D. C. *Inorg. Chem.* 1989, *28*, 2355.

[4] Evans, C. J.; Karpel, S. *J. Organomet. Chem. Libr.* 1985, *16*, 1.

[5] Lockhart, T. P.; Calabrese, J. C.; Davidson, F. *Organometallics* 1987, *6*, 2479.

[6] Chandresekhar, V.; Day, R. O.; Holmes, J. M.; Holmes, R. R. *Inorg. Chem.* 1988, *27*, 958.

[7] Ng, S. W.; Kumar Das, V. G.; Skelton, B. W.; White, A. H. *J. Organomet. Chem.* 1989, *377*, 221.

[8] Ng, S. W.; Kumar Das, V. G.; Yip, W.-H.; Wang, R.-J.; Mak, T. C. W. *J. Organomet. Chem.* 1990, *393*, 201.

0276-7333/92/2311-2206$03.00/0

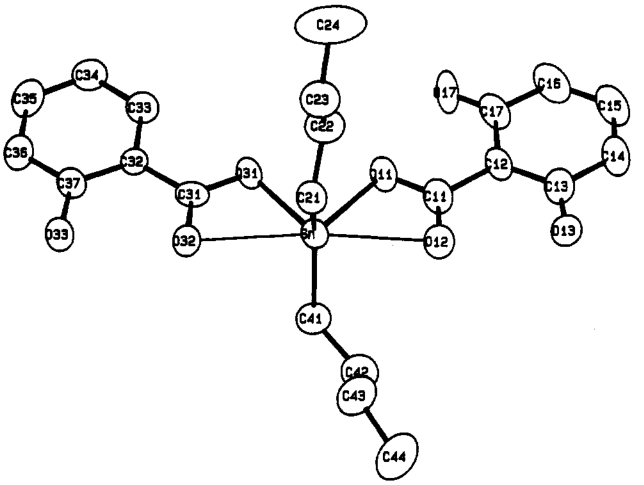

Figure 1. ORTEP plot of $(n\text{-Bu})_2Sn(O_2CC_6H_4\text{-}o\text{-}OH)_2$ (1) with thermal ellipsoids at the 30% probability level. Hydrogen atoms are omitted for clarity. Long Sn–O bonds are shown as narrow lines. Both positions for the oxygen atom of the disordered OH group (O13 and O17) are shown.

Preparation of $(n\text{-Bu})_2Sn(O_2CC_6H_4\text{-}o\text{-}X)_2$: X = OH (1); X = Cl (2). Di-*n*-butyltin(IV) oxide (2.0 g, 8.03 mmol) was added to *o*-hydroxybenzoic acid (2.22 g, 16.0 mmol) or *o*-chlorobenzoic acid (2.50 g, 16.0 mmol), and the mixture so obtained was refluxed in benzene (50 mL) for 4 h using a Dean Stark distillation apparatus. Water formed in the reaction was removed azeotropically. The solvent was evaporated and the residue extracted with petroleum ether (40–60 °C). The crude product was recrystallized from a mixture of dichloromethane and petroleum ether (40–60 °C).

Anal. Calcd for $C_{22}H_{28}O_6Sn$: C, 52.07; H, 5.52; Sn, 23.47. Found: C, 52.10; H, 5.68; Sn, 23.09. Mp 77 °C (yield 91%). MS: [*m*/*z*, assignment, rel intensity %] 508 (M^+ for $C_{22}H_{28}O_6Sn$, 1.3), 371 (M^+ $^-OC(O)C_6H_4OH$, 78.3); 270 (M^+ $^-C_4H_9[OC(O)]_2C_6H_4OH$, 8.9); 257 ($M^+$ $^-(C_4H_9)_2OC(O)C_6H_4OH$, 41.3); 213 ($M^+$ $^-(C_4H_9)_2$-$[OC(O)]_2C_6H_4OH$, 100).

Anal. Calcd for $C_{22}H_{26}O_4Cl_2Sn$: C, 48.53; H, 4.78; Cl, 13.05; Sn, 21.87. Found: C, 48.60; H, 5.01; Cl, 12.83; Sn, 21.22. Mp 78 °C (yield 90%). MS: [*m*/*z*, assignment, rel intensity %] 544 (M^+ for $C_{22}H_{26}O_4Cl_2Sn$, 0.06); 487 (M^+ $^-C_4H_9$, 83.3); 411 (M^+ $^-C_4H_9{\cdot}C_3H_5{\cdot}Cl$, 4.5); 389 ($M^+$ $^-OC(O)C_6H_4Cl$, 16.6); 367 (M^+ $^-C_4H_9{\cdot}C_3H_5{\cdot}OC(O)Cl$, 30.8); 276 ($M^+$ $^-C_4H_9{\cdot}C_4H_8OC(O)C_6H_4Cl$, 100); 139 ($M^+$ $^-C_4H_9)_2SnOC(O)O{\cdot}C_6H_4Cl$, 35.9).

X-ray Studies. All X-ray crystallographic studies were done using an Enraf-Nonius CAD4 diffractometer and graphite-monochromated molybdenum radiation ($\lambda K\bar{\alpha}$ = 0.710 73Å) at an ambient temperature of 23 ● 2 °C. Details of the experimental procedures have been described previously.[9]

Crystals were mounted in thin-walled glass capillaries which were sealed as a precaution against moisture sensitivity. Data were collected using the θ–2θ scan mode. Empirical absorption corrections based on ψ scans were applied (relative transmission factors on I from 0.9542 to 0.9996 for 1 and from 0.8696 to 0.9992 for 2). The structures were solved by use of Patterson and difference Fourier techniques and were refined by full-matrix least squares.[10]

All computations were performed on a Microvax II computer using the Enraf-Nonius SDP system of programs.

X-ray Study for $(n\text{-Bu})_2Sn(O_2CC_6H_4\text{-}o\text{-}OH)_2$ (1). Crystals of 1 are colorless intergrown laths. Pieces cut for the X-ray study were either polycrystalline or somewhat small. The crystal used for the study had dimensions of 0.13 × 0.18 × 0.43 mm.

Crystal Data for 1: $C_{22}H_{28}O_6Sn$, monoclinic space group $P2_1/c$ (C_{2h}^5, No. 14),[11] a = 9.345 (3) Å, b = 24.086 (5) Å, c = 10.839 (3) Å, β = 107.77 (2)°, Z = 4, and $\mu_{MoK\bar{\alpha}}$ = 11.329 cm^{-1}. A total of 2655 independent reflections ($+h,+k,\pm l$; $3° \leq 2\theta_{MoK\bar{\alpha}} \leq 43°$) was collected.

Table I. Atomic Coordinates in Crystalline $(n\text{-Bu})_2Sn(O_2CC_6H_4\text{-}o\text{-}OH)_2$ (1)[a]

atom[b]	x	y	z	B(equiv),[c] Å^2
Sn	0.05828 (6)	0.07303 (2)	0.20347 (5)	4.45 (1)
O11	−0.0028 (6)	0.0957 (2)	0.0055 (5)	5.4 (1)
O12	0.1941 (6)	0.1454 (2)	0.1053 (5)	5.9 (1)
O13	0.2914 (8)	0.2169 (4)	−0.0329 (7)	5.6 (2)
O17	−0.115 (2)	0.1096 (8)	−0.235 (2)	7.2 (5)
O31	−0.1328 (5)	0.0229 (2)	0.1354 (4)	4.8 (1)
O32	−0.0480 (5)	0.0051 (2)	0.3442 (5)	5.2 (1)
O33	−0.1828 (6)	−0.0690 (3)	0.4474 (5)	5.9 (1)
C11	0.0961 (8)	0.1324 (3)	0.0044 (7)	5.0 (2)
C12	0.0854 (8)	0.1594 (3)	−0.1215 (7)	4.8 (2)
C13	0.1905 (9)	0.1999 (4)	−0.1274 (8)	6.0 (2)
C14	0.180 (1)	0.2235 (4)	−0.2476 (8)	7.1 (2)
C15	0.071 (1)	0.2083 (4)	−0.3551 (8)	7.5 (3)
C16	−0.033 (1)	0.1673 (4)	−0.3503 (8)	7.2 (3)
C17	−0.0293 (9)	0.1416 (4)	−0.2361 (7)	5.6 (2)
C21	−0.0211 (8)	0.1403 (4)	0.2909 (7)	5.1 (2)
C22	−0.160 (1)	0.1668 (4)	0.1999 (9)	6.7 (3)
C23	−0.220 (1)	0.2130 (4)	0.2636 (9)	7.5 (3)
C24	−0.365 (2)	0.2371 (6)	0.172 (2)	15.7 (5)
C31	−0.1423 (8)	−0.0036 (3)	0.2366 (7)	4.4 (2)
C32	−0.2673 (7)	−0.0427 (3)	0.2217 (6)	4.0 (2)
C33	−0.3740 (9)	−0.0499 (4)	0.1008 (7)	5.2 (2)
C34	−0.4926 (9)	−0.0857 (4)	0.0839 (8)	5.8 (2)
C35	−0.5026 (9)	−0.1166 (4)	0.1880 (9)	6.5 (2)
C36	−0.3970 (9)	−0.1113 (4)	0.3076 (8)	5.8 (2)
C37	−0.2811 (8)	−0.0741 (3)	0.3256 (7)	4.7 (2)
C41	0.2371 (9)	0.0167 (4)	0.2280 (8)	5.9 (2)
C42	0.395 (1)	0.0392 (5)	0.2657 (9)	7.5 (3)
C43	0.441 (1)	0.0723 (5)	0.381 (1)	8.1 (3)
C44	0.607 (1)	0.0875 (6)	0.425 (1)	10.7 (4)

[a] Numbers in parentheses are estimated standard deviations. [b] Atoms are labeled to agree with Figure 1. [c] Equivalent isotropic thermal parameters are calculated as $^4/_3[a^2\beta_{11} + b^2\beta_{22} + c^2\beta_{33} + ab(\cos\gamma)\beta_{12} + ac(\cos\beta)\beta_{13} + bc(\cos\alpha)\beta_{23}]$.

During solution of the structure, it became apparent that there was positional disorder in one of the hydroxy phenyl groups with two distinct positions for the hydroxy oxygen atom. The occupancy for these partial atoms was refined to 0.32 for O17 and 0.68 for O13 (Figure 1).

All non-hydrogen atoms were subsequently refined anisotropically. All but the hydroxyl hydrogen atoms were included in the refinement as fixed isotropic scatterers in ideal positions. Hydroxyl hydrogen atom positions for O13 and O33 were obtained from a difference Fourier synthesis. These atoms (H1 and H2, respectively) were also treated as fixed isotropic scatterers. The final agreement factors[12] were R = 0.038 and R_w = 0.048 for the 1705 reflections with $I \geq 3\sigma_I$.

X-ray Study for $(n\text{-Bu})_2Sn(O_2CC_6H_4\text{-}o\text{-}Cl)_2$ (2). Colorless crystals of 2 are facetless with rounded edges and etched surfaces. The somewhat irregular crystal used for the study was cut to approximate dimensions of 0.45 × 0.50 × 0.53 mm.

Crystal Data for 2: $C_{22}H_{26}O_4Cl_2Sn$, monoclinic space group $P2_1/c$, a = 12.369 (2) Å, b = 8.830 (2) Å, c = 22.114 (5) Å, β = 102.18 (2)°, Z = 4, and $\mu_{MoK\bar{\alpha}}$ = 13.365 cm^{-1}. A total of 4136 independent reflections ($+h,+k,\pm l$; $3° \leq 2\theta_{MoK\bar{\alpha}} \leq 50°$) was collected.

Non-hydrogen atoms were refined anisotropically. Hydrogen atoms were included as fixed isotropic scatterers in ideal positions. The final agreement factors[12] were R = 0.028 and R_w = 0.042 for the 3330 reflections with $I \geq 3\sigma_I$.

Results

The atom-labeling scheme for 1 is shown in the ORTEP plot of Figure 1, while atomic coordinates and important bond lengths and angles are given in Tables I and II, respectively. The analogous information for 2 is given in

---

[9] Sau, A. C.; Day, R. O.; Holmes, R. R. *Inorg. Chem.* **1981**, *20*, 3076.

[10] The function minimized was $\sum w(|F_o| - |F_c|)^2$, where $w^{1/2} = 2F_oLp/\sigma_I$.

[11] *International Tables for X-ray Crystallography*; Kynoch: Birmingham, England, 1969; Vol. I, p 99.

[12] $R = \sum||F_o| - |F_c||/\sum|F_o|$ and $R_w = \{\sum w(|F_o| - |F_c|)^2/\sum w|F_o|^2\}^{1/2}$.

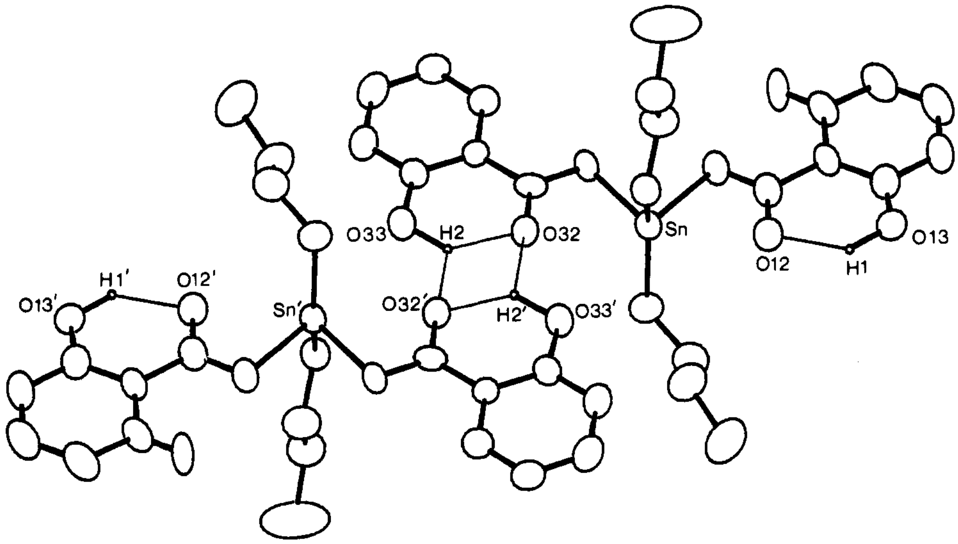

Figure 2. ORTEP plot of 1 including an inversion-related molecule ($-x$, $-y$, $1 - z$) to show the hydrogen-bonding interactions (narrow lines). The remaining hydrogen atoms are omitted for clarity.

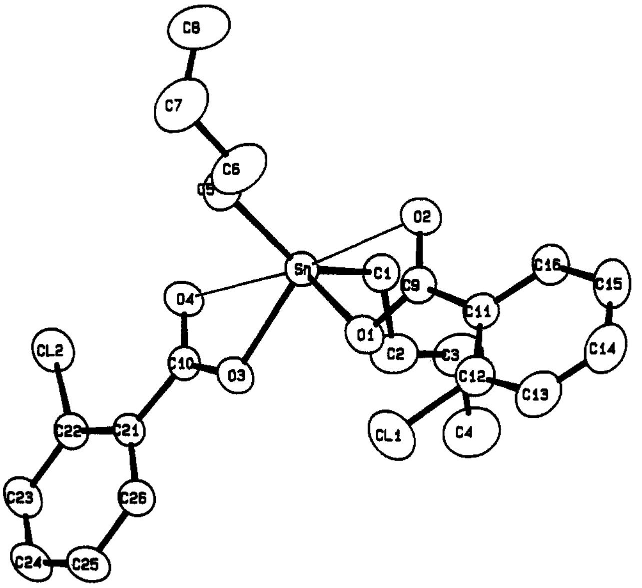

Figure 3. ORTEP plot of $(n\text{-Bu})_2Sn(O_2CC_6H_4\text{-}o\text{-}Cl)_2$ (2) with thermal ellipsoids at the 30% probability level. Hydrogen atoms are omitted for clarity. Long Sn–O bonds are shown as narrow lines.

Table II. Selected Distances (Å) and Angles (deg) for $(n\text{-Bu})_2Sn(O_2CC_6H_4\text{-}o\text{-}OH)_2$ (1)[a]

Sn–O11	2.117 (5)	Sn–C21	2.122 (9)
Sn–O12	2.570 (6)	Sn–C41	2.105 (9)
Sn–O31	2.095 (5)	O32–O33′	3.025 (7)
Sn–O32	2.630 (6)		
C11–O11	1.28 (1)	C31–O31	1.294 (9)
C11–O12	1.233 (8)	C31–O32	1.246 (8)
O11–Sn–O12	54.5 (2)	O12–Sn–C41	90.9 (3)
O11–Sn–O31	81.6 (2)	O31–Sn–O32	54.1 (2)
O11–Sn–O32	135.7 (2)	O31–Sn–C21	102.8 (3)
O11–Sn–C21	103.5 (3)	O31–Sn–C41	103.4 (3)
O11–Sn–C41	104.6 (3)	O32–Sn–C21	88.3 (3)
O12–Sn–O31	136.1 (2)	O32–Sn–C41	87.2 (3)
O12–Sn–O32	169.7 (1)	C21–Sn–C41	143.9 (3)
O12–Sn–C21	87.2 (3)	Sn–O11–C11	102.4 (4)
		Sn–O31–C31	104.9 (4)

[a] Estimated standard deviations are given in parentheses. The atom-labeling scheme is shown in Figure 1.

Table III. Atomic Coordinates in Crystalline $(n\text{-Bu})_2Sn(O_2CC_6H_4\text{-}o\text{-}Cl)_2$ (2)[a]

atom[b]	x	y	z	B(equiv),[c] Å^2
Sn	0.61463 (2)	0.08750 (3)	0.60060 (1)	4.314 (5)
Cl1	0.7553 (1)	0.3500 (2)	0.79861 (6)	8.50 (3)
Cl2	0.17290 (8)	0.0606 (1)	0.48654 (5)	6.77 (2)
O1	0.6959 (2)	0.1603 (3)	0.6901 (1)	5.55 (5)
O2	0.8248 (2)	0.0773 (3)	0.6434 (1)	6.02 (6)
O3	0.4751 (2)	0.1607 (3)	0.6329 (1)	5.14 (5)
O4	0.4090 (2)	0.0706 (3)	0.5409 (1)	5.27 (6)
C1	0.6154 (3)	−0.1524 (5)	0.6095 (2)	5.37 (8)
C2	0.5492 (4)	−0.2120 (5)	0.6529 (2)	7.2 (1)
C3	0.5618 (4)	−0.3836 (6)	0.6629 (2)	8.5 (1)
C4	0.4944 (5)	−0.4500 (6)	0.7036 (3)	10.0 (2)
C5	0.6348 (3)	0.2588 (5)	0.5362 (2)	5.89 (9)
C6	0.7263 (4)	0.3674 (6)	0.5546 (2)	9.0 (1)
C7	0.7373 (4)	0.4764 (6)	0.5017 (3)	9.6 (1)
C8	0.7871 (6)	0.4102 (8)	0.4568 (3)	15.0 (2)
C9	0.7981 (3)	0.1301 (4)	0.6904 (2)	4.70 (7)
C10	0.3929 (2)	0.1311 (4)	0.5885 (1)	4.18 (6)
C11	0.8831 (2)	0.1527 (4)	0.7485 (1)	4.50 (7)
C12	0.8716 (3)	0.2434 (4)	0.7978 (2)	5.43 (8)
C13	0.9582 (4)	0.2544 (5)	0.8500 (2)	7.0 (1)
C14	1.0543 (3)	0.1774 (6)	0.8520 (2)	7.3 (1)
C15	1.0673 (3)	0.0885 (5)	0.8034 (2)	7.2 (1)
C16	0.9839 (3)	0.0763 (5)	0.7521 (2)	5.88 (9)
C21	0.2815 (2)	0.1711 (4)	0.5996 (1)	4.04 (6)
C22	0.1818 (3)	0.1444 (4)	0.5593 (2)	4.72 (7)
C23	0.0810 (3)	0.1839 (5)	0.5741 (2)	6.03 (9)
C24	0.0797 (3)	0.2524 (5)	0.6282 (2)	6.9 (1)
C25	0.1779 (3)	0.2821 (5)	0.6705 (2)	6.45 (9)
C26	0.2771 (3)	0.2400 (4)	0.6554 (2)	5.22 (8)

[a] Numbers in parentheses are estimated standard deviations. [b] Atoms are labeled to agree with Figure 3. [c] Equivalent isotropic thermal parameters are calculated as $^4/_3[a^2\beta_{11} + b^2\beta_{22} + c^2\beta_{33} + ab(\cos\gamma)\beta_{12} + ac(\cos\beta)\beta_{13} + bc(\cos\alpha)\beta_{23}]$.

Figure 3 and in Tables III and IV. Anisotropic thermal parameters, additional bond lengths and angles, and hydrogen atom parameters for both compounds are provided as supplementary material.

Discussion

Synthesis. Compounds 1 and 2 isolated from dehydration reactions between di-*n*-butyltin(IV) oxide and *o*-hydroxybenzoic acid and *o*-chlorobenzoic acid, respectively, in the molar ratio 1:2 are white crystalline solids soluble in organic solvents. Elemental analyses and mass spectral data reveal the composition of these compounds to be $(n\text{-Bu})_2Sn(O_2CC_6H_4\text{-}o\text{-}X)_2$, where X = OH (1) and Cl (2).

Table IV. Selected Distances (Å) and Angles (deg) for $(n\text{-Bu})_2Sn(O_2CC_6H_4\text{-}o\text{-}Cl)_2$ (2)[a]

Sn–O1	2.122 (2)	Sn–O4′	3.381 (2)
Sn–O2	2.574 (2)	Sn–C1	2.127 (4)
Sn–O3	2.104 (2)	Sn–C5	2.128 (4)
Sn–O4	2.612 (2)		
O1–C9	1.290 (4)	O3–C10	1.282 (3)
O2–C9	1.247 (4)	O4–C10	1.235 (4)
O1–Sn–O2	54.88 (8)	O3–Sn–O4′	121.59 (6)
O1–Sn–O3	81.46 (8)	O3–Sn–C1	105.2 (1)
O1–Sn–O4	135.11 (8)	O3–Sn–O4	53.70 (8)
O1–Sn–O4′	156.85 (7)	O3–Sn–C5	103.2 (1)
O1–Sn–C1	102.9 (1)	O4–Sn–O4′	67.89 (6)
O1–Sn–C5	108.0 (1)	O4–Sn–C1	88.5 (1)
O2–Sn–O3	136.34 (8)	O4–Sn–C5	86.7 (1)
O2–Sn–O4	169.89 (8)	O4′–Sn–C1	70.9 (1)
O2–Sn–O4′	102.06 (7)	O4′–Sn–C5	71.0 (1)
O2–Sn–C1	87.0 (1)	C1–Sn–C5	140.4 (1)
O2–Sn–C5	91.1 (1)	Sn–O4–Sn′	112.11 (8)
Sn–O2–C9	82.4 (2)	Sn–O4–C10	81.9 (2)
Sn–O1–C9	102.3 (2)	Sn′–O4–C10	166.0 (2)
Sn–O3–C10	104.6 (2)		

[a] Estimated standard deviations are given in parentheses. The atom-labeling scheme is shown in Figure 3.

Solid-State Structures. When only intramolecular interactions are considered, the geometry about the tin atom in both 1 and 2 is very similiar and similar to that found in other diorganotin dicarboxylates, e.g., B–D.[6–8] Although this geometry has been described as skew trapezoidal bipyramidal,[8] it is, perhaps, at least as useful to refer it to a bicapped tetrahedron.[6] For both compounds, there are four normal covalent bonds to tin (Sn–O or Sn–C bond lengths from 2.095 (4) to 2.128 (4) Å and two longer dative $Sn–O_{acyl}$ bonds (2.570 (6) to 2.630 (6) Å). The former define the tetrahedra and the latter the capped faces.

For 1, the atoms forming the tetrahedron (C21, C41, O11, and O31) form four "normal" tetrahedral O–Sn–C (102.8 (3)–104.6 (3)°) and form two angles that show, at least in part, the effect of the capping atoms (O–Sn–O = 81.6 (2)° and C–Sn–C = 143.9 (3)°). For 2, these parameters are for C1, C5, O1, and O3: O–Sn–C, 102.9 (1)–108.0 (1)°, O–Sn–O = 81.46 (8)°, and C–Sn–C = 140.4 (1)°.

Both 1 and 2 exist in the solid state as weakly connected dimers (Figures 2 and 4). In the case of 2, the intermolecular interaction involves the tin atom and the acyl oxygen atom of an inversion related molecule with which a four-membered Sn–O–Sn–O ring is formed (Figure 4). The intermolecular Sn–O distance of 3.381 (2) Å is considerably longer than the covalent sum of 2.13 Å but shorter than the van der Waals' sum of 3.70 Å.[13]

This type of intermolecular interaction is the same as that which has been observed in the isomorphous o-bromobenzoate derivative D[8] where the intermolecular Sn–O distance is 3.451 (5) Å; thus, the electronegativity effect of substitution of chlorine in place of bromine does not result in any significant structural change. Including the intermolecular interaction, the coordination of the tin in D has been referred to as pentagonal bipyramid[8] with an apical C–Sn–C angle of 140.5 (3)° and the sum of angles in the pentagonal plane of 360.0°. The sum of these angles for 2 is also 360.0°.[14]

These intermolecular Sn–O and long Sn–O intramolecular distances are listed in Table V along with C–Sn–C bond angles for the dicarboxylates 1, 2, and D–H,[8,15–18] forming "dimeric" structures. Similar data are given for the monomeric derivatives B[6] and C[7] for comparison.

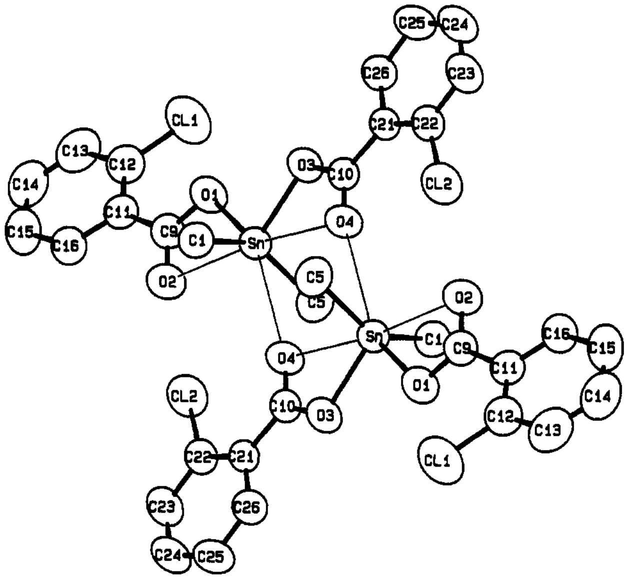

Figure 4. ORTEP plot of 2 including an inversion-related molecule (1 – x, –y, 1 – z) to show the weak intermolecular Sn–O interactions. Pendant atoms of the n-butyl groups are omitted for clarity.

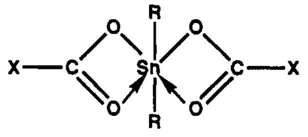

	R	X
E	n-Bu	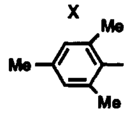
F	Me	Ph
G	Et	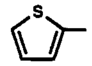
H	n-Bu	Ph-S-CH₂-

The pentagonal plane in 2 is part of a larger planar system, which involves both halves of the dimer. The 14-atom fragment which includes the tin atom, both carboxyl groups, and the o-chlorophenyl group containing Cl2 is planar to within ±0.056 (3) Å. The inversion-related O4 is displaced from the mean plane by only 0.051 (3) Å. Since inversion-related planes are required to be parallel, the plane of the 14 inversion-related atoms is essentially coincident, and dimer has a 28-atom nearly-planar fragment. The o-chlorophenyl groups containing Cl1 are rotated out of this plane by about 20°. The torsion angle O1–C9–C11–C12 is –20.1 (5)°. Alternatively, the dihedral angle between the plane defined by C9, C11–C16, Cl1 and the molecular plane is 19.1 (1)°.

The intermolecular interaction in 1 is driven by the hydrogen-bonding capability of the o-hydroxy groups.

---

(13) Huheey, J. E. *Inorganic Chemistry*, 3rd ed.; Harper and Row: New York, 1983.

(14) The two compounds 2 and D[8] are isomorphous. The coordinates reported in the literature[8] for D can be made analogous to those reported here by the transformation (x, $^1/_2 - y$, $^1/_2 + z$). It is noted that the lattice constants are nearly identical.

(15) Garbauskas, M. F.; Wengrovius, J. H. *Acta. Crystallogr.* **1991**, *C47*, 1969.

(16) Tiekink, E. R. T. *J. Organomet. Chem.* **1991**, *408*, 323.

(17) Vatsa, C.; Jain, V. K.; Kesavadas, T.; Tiekink, E. R. T. *J. Organomet. Chem.* **1991**, *410*, 135.

(18) Sandhu, G. K.; Sharma, N.; Tiekink, E. R. T. *J. Organomet. Chem.* **1989**, *371*, C1.

Table V. Comparison of X-ray Structural Parameters for Dicarboxylate Tin Derivatives

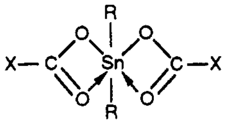

compd	Sn---O_{inter}, Å	C–Sn–C, deg	short Sn–O_{intra},[a] Å	long Sn–O_{intra},[a] Å	ref
		OH Hydrogen-Bonded Dimer			
1, R = *n*-Bu	3.605 (5)	143.9 (3)	2.117 (5)	2.570 (6)	this work
X = 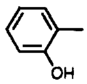			2.095 (5)	2.630 (6)[b]	
		Sn_2O_2 Monomer-to-Dimer Formation			
C, R = *n*-Bu		130.6 (2)	2.075 (3)[c]	2.635 (4)[c]	7
X = 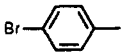					
B,[d] R = Me		134.7 (2)	2.077 (3)	2.556 (3)	6
X = 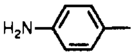			2.097 (3)	2.543 (3)	
H, R = *n*-Bu		140.7 (2)	2.134 (4)[c]	2.559 (5)[c]	18
X = $PhSCH_2$–					
D, R = *n*-Bu	3.451 (5)	140.5 (3)	2.097 (4)	2.617 (5)	8
X = 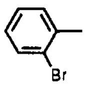			2.095 (5)	2.608 (5)[b]	
2, R = *n*-Bu	3.381 (2)	140.4 (1)	2.122 (2)	2.574 (2)	this work
X = 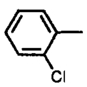			2.104 (2)	2.612 (2)[b]	
I(II),[e] R = *n*-Bu	3.134	144.5 (3)	2.130 (6)	2.575 (8)	22
X = –$C(Et)_2$–			2.144 (7)	2.515 (7)[b]	
E, R = *n*-Bu	3.148	145.4 (5)	2.088 (9)	2.451 (6)	15
X = 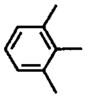			2.116 (9)	2.651 (9)[b]	
F, R = Me	2.96 (1)	147.2 (7)	2.128 (8)	2.510 (9)	16
X = Ph			2.156 (9)	2.51 (1)[b]	
G, R = Et	2.891 (6)	151.7 (4)	2.129 (5)	2.473 (5)	17
X = 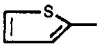			2.143 (5)	2.556 (5)[b]	
I(I),[e] R = *n*-Bu	2.775	158.8 (2)	2.159 (5)	2.465 (6)	22
X = –$C(Et)_2$–			2.140 (6)	2.655 (7)	

[a] The first listed short and long Sn–O intramolecular distances for each entry correspond to oxygen atoms of the same ring. The second listings also are paired entries for the other carboxylate ring. [b] The oxygen atom associated with this distance is the one used in forming the weak dimeric arrangements. Column 2 lists the resulting Sn–O intermolecular distance. [c] Only one crystallographically-independent ring is present since the monomeric molecule lies on a 2-fold rotation axis passing through the tin atom. [d] Intermolecular contacts for B suggest N–H---O hydrogen bonding. [e] Phases I and II of $[(n\text{-}Bu_2)Sn(\text{diethylmalonate})]_x$ (I). Bond parameters are from our calculations using the atomic coordinates and cell constants supplied in ref 23.

Thus, 1 is unique in contrast to the other derivatives in Table V that exhibit dimeric interactions. The hydroxyl hydrogen atoms which are adjacent to the acyl oxygen atoms enter into intramolecular hydrogen-bonding interactions with these atoms to form six-membered rings (Figure 2). In addition to these interactions, the six-membered ring containing O32 and O33 is in proximity to its inversion-related ring in such a way that bifurcated hydrogen bonds connecting inversion-related O32 atoms form a four-membered H–O–H–O ring. This arrangement places the tin atoms at a distance of 3.605 (5) Å from inversion-related O33 atoms, which is only very slightly shorter than the van der Waals' sum. However, in view of the correlation discussed below, the rather large C–Sn–C angle of 143.9 (3) Å appears to result from a van der Waals' alignment attributable to the nearby hydrogen-bonded phenolate unit.

The monomeric units in 1 are essentially planar except for the atoms of the butyl groups. The atoms comprising the hydroxyphenyl carboxylates and the tin atom are coplanar to within ±0.086 (9) Å. The two halves of the dimer, in this case, are not coplanar. The two parallel planes are separated by about 0.5 Å as judged from the displacement of the inversion-related O33 atom of 0.542 (4) Å from the parent plane.

In the related monomeric solids, dimethyltin bis(*p*-aminobenzoate) (B)[6] and di-*n*-butyltin bis(*p*-bromobenzoate) (C),[7] where there are *no* intermolecular Sn–O interactions, the C–Sn–C angles are 134.7 (2) and 130.6 (2)°, respectively (Table V). In the dimeric ortho-halogen compounds 2 and D–G, the angles are larger than 140°, presumably due to the intermolecular Sn–O interactions. In fact, as evident in Table V, the C–Sn–C angle increases uniformly as the intermolecular Sn–O distance responsible for dimer formation decreases. This is in keeping with the approach toward a distorted pentagonal bipyramid arrangement as a seventh "bond" forms at the tin center. Whether Sn–O_{inter} is considered a bond or not for any of these diorganotin derivatives is a semantic question.

However, this distance for G is already over 50% of the change in length on going from the van der Waals' sum to the covalent Sn–O sum. The correlation expressed in Table V dispels uncertainty in the literature[16,17] regarding the influence of the Sn–O intermolecular interaction on the geometry at tin.

Spectral Data. In addition to the X-ray structure found for 1, other possible formulations involving hydrogen bonding are the monomeric and polymeric assemblies, a and b, exhibiting one kind and two kinds of hydrogen bonds, respectively. Examination of the infrared spectra of the *o*-hydroxybenzoate derivative 1 (in KBr) reveals three absorptions at 3150, 3090, and 3040 cm^{-1}, assignable as OH stretching modes. The presence of these modes is consistent with the solid-state structure of 1 (Figure 2) showing three kinds of hydrogen bonds, the strongest of which is associated with the intramolecular O33–H2- - -O32 interaction. A H2- - -O32 distance of 1.688 (6) Å was obtained. The weakest hydrogen bond is the one formed in creating the dimeric unit via O33—H2- - -O32′ and O33′–H2′- - -O32 intermolecular interactions. The hydrogen-bond distance here is H2- - -O32′ equal to 2.416 (5) Å. The intramolecular hydrogen-bonding interaction O13–H1- - -O12 of the *o*-hydroxybenzoate not involved in the weak dimer formation has a hydrogen-bond distance H1- - -O12 of 1.775 (6) Å. For the *o*-chlorobenzoate 2, carbonyl stretching frequencies in the infrared assigned at 1605 and 1370 cm^{-1} are indicative of carboxyl group coordination.[19,20]

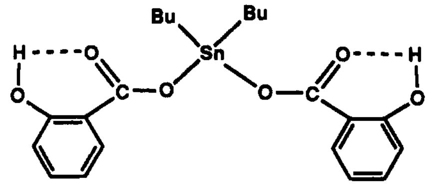

a

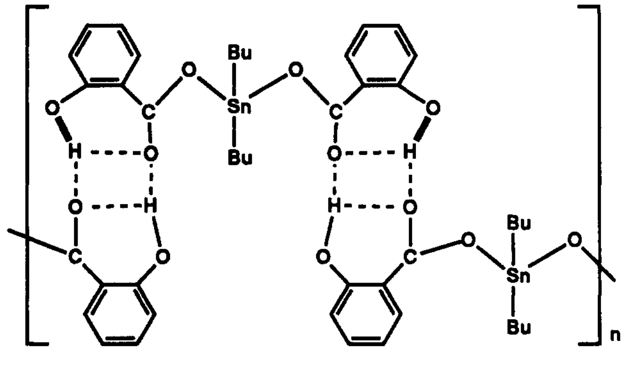

b

^{119m}Sn Mössbauer spectra show isomer shifts (s) and quadrupole splittings (q.s.) in mm s^{-1} at 1.47 and 3.57, respectively, for 1 and at 1.48 and 3.53, respectively, for 2. The ratio (ρ = q.s./δ $\sim$ 2.4) suggests that the tin atoms in the compounds have a coordination number greater than 4[21] in both cases. With the availability of C–Sn–C bond angles from the X-ray studies reported here, quadrupole splitting values can also be calculated using the Sham and Bancroft equation.[22] The values obtained (3.53 for 1 and 3.45 for 2 mm s^{-1}) are in good agreement with the experimental values (3.57 for 1 and 3.53 for 2 mm s^{-1}). Thus, both the infrared and ^{119m}Sn Mössbauer data of 1 and 2 are consistent with the molecular structures established by X-ray analysis in that carboxyl group chelation is supported.

It is interesting to compare the structures at tin for the compounds listed in Table V with a recent report of the structures of three crystalline phases of $[(n\text{-Bu})_2\text{Sn(diethylmalonate)}]_x$[23] (I) appearing as linear polymers with dicarboxylate ligands bridging tin atoms. Like the compounds in Table V derived from monocarboxylic acids, the three phases of the diethylmalonate derivative have trans-oriented butyl groups attached to a highly-distorted octahedral tin atom that has two short and two long Sn–O linkages per tin atom. These distances are in the ranges 2.07–2.27 and 2.47–2.66 Å, respectively.[23] These ranges compare with 2.08–2.16 Å for the short Sn–O distances and 2.45–2.65 Å for the long Sn–O distances for the similarly structured dicarboxylates listed in Table V. Hence, the structural integrity at the tin atoms is maintained in both sets of compounds independent of whether they are derived from mono- or dicarboxylic acids. Further, the correlation between the Sn–O intermolecular distance and the C–Sn–C angle cited for the compounds in Table V is maintained.

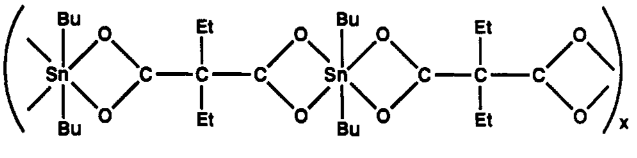

I

Acknowledgment. S.K.B. and Y.S. are grateful to UGC (India) for teacher and Senior Fellowships. These authors also thank Bhabba Atomic Research Centre (Bombay) for use of Mössbauer facilities. R.R.H. gratefully acknowledges the support provided by the donors of the Petroleum Research Fund, administered by the American Chemical Society.

Supplementary Material Available: Tables of thermal parameters, additional bond lengths and angles, and hydrogen atom parameters (Tables S1–S3 for 1, Tables S4–S6 for 2, respectively) (12 pages). Ordering information is given on any current masthead page.

OM910682M

---

(19) Nakamoto, K. *Infrared and Raman Spectra of Inorganic and Coordination Compounds*, 3rd ed.; Wiley Interscience: New York, 1978; 230ff.

(20) Vollano, J. F.; Day, R. O.; Rau, D. N.; Chandrasekhar, V.; Holmes, R. R. *Inorg. Chem.* **1984**, *23*, 3153.

(21) Herber, R. H.; Stöckler, H. A.; Reichle, W. T. *J. Chem. Phys.* **1965**, *42*, 2447.

(22) Sham, T. K.; Bancroft, G. M. *Inorg. Chem.* **1975**, *14*, 2281.

(23) Wengrovius, J. H.; Garbauskas, M. F. *Organometallics* **1992**, *11*, 1334.